ULTRASENSITIVE FLUORESCENCE DETERMINATION OF 6-THIOGUANINE IN BIOLOGICAL SAMPLES BASED ON THE SILVER NANOPARTICLE-MEDIATED RELEASE OF ACRIDINE ORANGE PROBE**

V. K. Verma, K. Tapadia*, T. Maharana, A. Sharma

Department of Chemistry, National Institute of Technology, CG, 492010, Raipur, India; e-mail: ktapadia.chy@nitrr.ac.in

This article reports a simple, convenient, and very sensitive method for the determination of 6-thioguanine (6-TG). The basic phenomenon in the proposed method is fluorescence resonance energy transfer, where acridine orange (AO) act as a donor and citrate-stabilized silver nanoparticles (AgNPs) as an acceptor. A noncovalent bond between the surfaces of AgNPs and AO was found, and the effect of fluorescence quenching was observed. The fluorescence spectra of AO recovered after further addition of 6-TG are responsible for the aggregation of AgNPs. Under ideal conditions, the linear relationship of 6-TG in the concentration range of 0.005 to 0.04 μM was displayed, and the limit of detection of 6-TG was obtained as 5.3 nM. Under ideal conditions, the linear relationship of 6-TG was displayed in the concentration range of 0.005 to 0.04 μM, and the limit of detection of 6-TG was obtained as 5.3 nM. The proposed method offers a rapid analysis to determine 6-TG in human serum, blood, and urine samples.

Keywords: *fluorescence, silver nanoparticles, 6-thioguanine, acridine orange.*

СВЕРХЧУВСТВИТЕЛЬНОЕ ФЛУОРЕСЦЕНТНОЕ ОПРЕДЕЛЕНИЕ 6-ТИОГУАНИНА В БИОЛОГИЧЕСКИХ ОБРАЗЦАХ НА ОСНОВЕ ОПОСРЕДОВАННОГО НАНОЧАСТИЦАМИ СЕРЕБРА ВЫСВОБОЖДЕНИЯ ЗОНДА АКРИДИНОВОГО ОРАНЖЕВОГО

V. K. Verma, K. Tapadia*, T. Maharana, A. Sharma

УДК 535.372;620.3

Национальный технологический институт, Чхаттисгарх, 492010, Райпур, Индия; e-mail: ktapadia.chy@nitrr.ac.in

(Поступила 28 января 2019)

Представлен простой и чувствительный метод определения содержания 6-тиогуанина (6-TG). Метод основан на резонансном переносе энергии флуоресценции, при котором донором служит акридиновый оранжевый (АО), акцептором — стабилизированные цитратом наночастицы серебра (Ag-НЧ). Обнаружена нековалентная связь между поверхностями Ag-НЧ и АО, наблюдается эффект тушения флуоресценции. Спектры флуоресценции АО, регистрируемые после дальнейшего добавления 6-TG, свидетельствуют об агрегации Ag-НЧ. В идеальных условиях линейная зависимость имеет место в диапазоне концентраций 0.005—0.04 мкм, предел обнаружения 6-TG 5.3 нмоль. Метод дает возможность проведения экспресс-анализа содержания 6-TG в образцах сыворотки, крови и мочи человека.

Ключевые слова: *флуоресценция, наночастица серебра, 6-тиогуанин, акридиновый оранжевый.*

** Full text is published in JAS V. 87, No. 2 (http://springer.com/journal/10812) and in electronic version of ZhPS V. 87, No. 2 (http://www.elibrary.ru/title_about.asp?id=7318; sales@elibrary.ru).

Introduction. Thiopurine drugs, such as 6-thioguanine (6-TG; 2-amino-1,7-dihydro-6-*H*-purine), are antimetabolites. The nucleic acid guanine is one of the basic components [1, 2]. 6-TG has chemotherapeutic properties and is often used to treat acute lymphocytic leukemia, acute myeloid leukemia, and Crohn's disease, among others [3, 4]. 6-TG acts as an active metabolite in the liver by transforming to thioguanylic acid, thioguanosine phosphate derivatives, and their respective nucleotides within the cell. 6-TG increases the amount of thiopurine nucleotides into RNA and DNA, and apoptosis is often the end result [5–7]. The clinical tolerance of 6-TG has been found to be 250 pmol/8×10^8 in red blood cells [8]. This plausible dose also exhibits side effects that include bone marrow depression and gastrointestinal diseases [9]. Currently, several analytical methods are used as an assay for this purpose, such as high-performance liquid chromatography [7, 10], voltammetry [4], surface-enhanced Raman scattering [11], mass spectrometry [12, 13], localized surface plasmon resonance [14, 15], and electrochemical methods [16, 17]. These methods have their own pros and cons, including complications such as poor sensitivity and high cost. Therefore, a sensitive, rapid, and accurate method is required for quantitative analysis of 6-TG. Fluorescence resonance energy transfer (FRET) is relatively better than the previously mentioned methods because it is effective, economical, easy to perform, selective, sensitive, and allows real-time analysis. These advantages mean that FRET is one of the most powerful analytical techniques based on spectroscopy [18–20].

The energy-transfer technique is based on replacing the fluorophore (donor), with proximal ground state molecules (acceptor) through dipole–dipole interactions. The ground state of the donor and the excited state of the acceptor must overlap. The mutual distance of the donor–acceptor molecule should be 1–10 nm. Earlier FRET pairs were commonly found in organic dyes and fluorescent polymers, among others, but these polymers had some limitations, such as their narrow adsorption spectra, broad emission with long tails, and low quantum yield, which affected the efficiency of the FRET process. However, FRET can include metal nanoparticles (NPs), which allows one to overcome the specific drawbacks mentioned above. Thus, the FRET method using NPs is preferred in analytical and structural chemistry [21–24].

The progression of FRET using metal NPs has led to its great advantage of having no limitations, unlike other techniques [25, 26]. Among the metal NPs used in FRET, silver NPs (AgNPs) are promising because they can be employed in many applications due to their unique optical, chemical, and electronic properties. AgNPs produce an intense electronic absorption band in the visible region with higher extinction coefficients, tremendously elevated scattering quantum yield, and proficient quenching activity [27, 28]. Experimental evidences revealed that AgNPs are efficiently involved in FRET mechanism as a quenching agent. Fluorescence of several dyes was found to be aggregated due to the effective quenching property of AgNPs. The quenching process was probably caused by nonradiative energy transfer from the dye to AgNPs [29, 30].

The current study aims to develop a nanosensor system using acridine orange (AO) and AgNPs to determine 6-TG through the fluorescence activation mechanism.

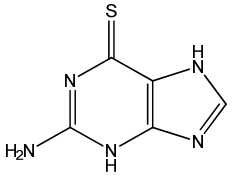

($C_5H_5N_5S$, WM-167.19 g/mol)
6-Thioguanine

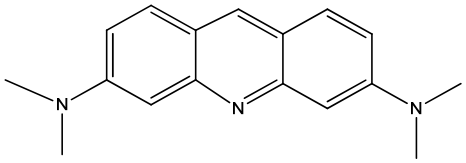

($C_{17}H_{19}N_3$, WM-265.36 g/mol)
Acridine orange

AO is an example of cationic dyes; thus, it adsorbs to the surface of citrate-capped AgNPs through electrostatic interaction. Since AgNPs have quenching abilities, AO's fluorescence was quenched because of the fluorescence resonance energy transfer to AgNPs. The formation of AO–AgNPs conjugating is preceded by the neutralization of charge. When 6-TG was added, AO's fluorescence was recovered, suggesting that the AO molecule was replaced from the AgNPs' surface. This was probably due to the Ag–S bond replacing the AO molecules. The proposed method was applied in a fluorescence recovery probe for determination of 6-TG at nanomolar levels in biological samples.

Experimental. All chemicals used were of analytical grade. Silver nitrate was obtained from Qualigens Fine Chemical, Fischer Scientific (Mumbai, India). AO and trisodium citrate were purchased from Loba Chemie (Mumbai, India), and thioguanine (6-TG) was purchased from Sigma Aldrich (St. Louis, MO, USA). The pH was adjusted by a 1.0 M concentration of sodium hydroxide and hydrochloric acid. Millipore water (Millipore, Billerica, MA, USA) was used for solution preparation in all experiments.

A G9800A fluorescence spectrophotometer (Agilent Technologies, Santa Clara, CA, USA) equipped with a 1.0×1.0 cm quartz cell was used for recording the fluorescence spectra of all samples. An UV-1800 UV-Visible spectrophotometer (Shimadzu, Kyoto, Japan) was used to measure absorption spectra. AgNP morphology was recorded by high-resolution transmission electron microscopy (HR-TEM, JEM-2100 G; JEOL, Tokyo Japan) using 200 kV for acceleration. The overall experiment was performed at room temperature.

Citrate-stabilized AgNPs were synthesized according to a method reported previously [31]; i.e., a 0.1 M solution of $AgNO_3$ was taken in a conical flask wrapped with foil paper and heated to its boiling temperature. After that, 5.0 mL of a 1% sodium citrate solution was added drop by drop to the solution under vigorous stirring. After further heating, a pale-yellow color appeared. The solution was then cooled at room temperature, followed by stirring. As a result, a dark-yellow color appeared, and finally the solution was stored in a dark brown bottle. The maximum absorbance of the prepared NPs was measured using an UV-Vis spectrophotometer. The shape and size of AgNPs were analyzed using HR-TEM, and the concentration of the synthesized AgNPs solution was obtained at 87.7 μM.

An Agilent G9800A fluorescence spectrophotometer was used to measure the fluorescence. A solution containing 300 μL of 0.1 M acetate buffer (pH ~5.0) was mixed to 100 μL of the synthesized AgNPs (10^{-3} μM). A further 200 μL of 10 μM AO was added to bring the total volume adjusted at 3.5 mL with Millipore water in a 5 mL volumetric flask. Afterwards, different concentrations of 6-TG were added and the solution further incubated for 20 min at room temperature. The fluorescence emission intensity (λ_{em}) of the mixture was measured in the absence (F_0) and presence (F) of 6-TG at 525-nm wavelength excitation (λ_{ex} ~ 450 nm) with the excitation and emission slits set to 5 nm. The difference between the two fluorescence signals depends on calibration and analysis.

According to optimum physiological conditions, appropriate samples of human urine, serum, and blood were used with the addition of a standard solution of 6-TG. Further, the sample was centrifuged at 3000 rpm for 20 min and diluted to 10 mL with deionized water. The required amount of the sample was taken for analysis.

Results and discussion. The maximum absorbance intensity of AgNPs with a characteristic plasmonic band was observed at λ_{max} ~ 415 nm [31]. The λ_{max} at 415 nm resembles an approximate size of NPs of 20–30 nm.

The particle size and shape of AgNPs were analyzed using HR-TEM (Fig. 1a). The prepared AgNPs were almost spherical in shape with a normal size of 20 ± 3 nm and the AgNPs concentration solution was estimated to be 87.7 μM.

The fluorescence quenching intensity of dye by AgNPs is due to fluorescence resonance energy transfer, electron transfer, and the inner filter effect. The efficiency of FRET depends upon the overlapping extent of the emission spectrum of donor fluorescence (ground state) with the acceptor absorption spectrum (excited energy level) [22]. In accordance to the FRET process, AO implements as a donor, while AgNP behaves as an acceptor (quencher). A partial overlap between the emission spectra of OA (λ_{em} ~ 525 nm) and the absorption spectrum of AgNPs (λ_{max} ~ 415 nm) signifies the occurrence of FRET between them (Fig. 2). The synthesized citrate-capped AgNPs have a negatively charged surface, while AO is a positively charged dye [32]. As AO is positively charged, it is absorbed on the AgNP negatively charged surface due to electrostatic interactions. Hence, the charge neutralization leads to the arrangement of a large AO–AgNPs cluster. The HR-TEM results for the AO–AgNPs assembly confirm this interaction. Thus, the FRET mechanism reveals that AO plays the role of donor and AgNPs acts as acceptor. The nonradiative energy transfer through AO leads to proficient fluorescence quenching by AgNPs. The emission spectra intensity of AO with AgNPs at several concentrations in the presence of acetate buffer (pH ~ 5.0) at room temperature was observed. The fluorescence intensities of AO were clearly quenched gradually on increasing the concentration of AgNPs. The quenching constant (K_{SV}) can be analyzed by the Stern–Volmer equation:

$$F/F_0 = 1 + K_{SV}[Q], \quad (1)$$

where F_0 and F are the fluorescence intensity in the absence and presence of AgNPs, respectively, and [Q] indicates the molar concentration of the quenching [33]. The quenching of AO's fluorescence by AgNPs was shown by the Stern–Volmer plot. The constant K_{SV} was used to calculate the starting linear plot at lower concentrations of AgNPs:

$$F/F_0 = 0.587[\text{AgNPs}] + 0.186, \; R^2 = 0.994. \quad (2)$$

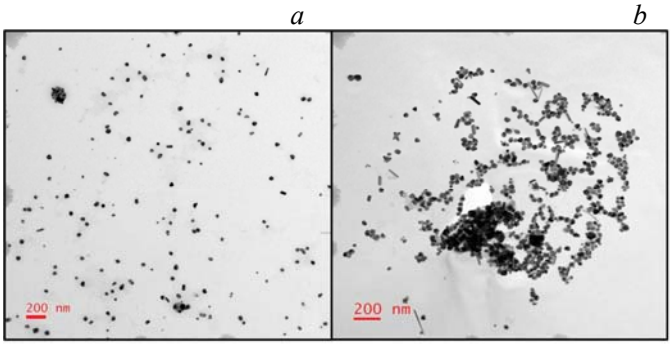

Fig. 1. HR-TEM image of AgNPs: (a) AgNPs (3.0×10^{-4} μM) with OA (0.57 μM), (b) AO–AgNPs in the presence of 0.03 μM 6-TG.

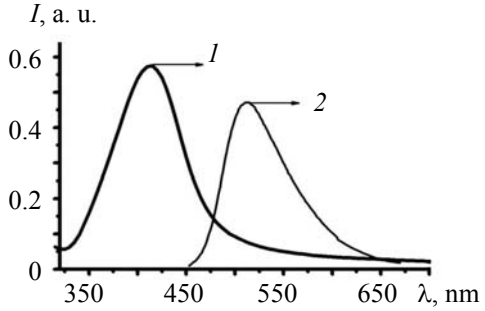

Fig. 2. Absorption spectrum of AgNPs (λ_{max} = 415 nm) (1) and fluorescence emission spectrum of AO (λ_{em} = 525 nm) (2).

The K_{SV} = 5.87 μM was obtained. Such a large K_{SV} value suggests the immense interaction between AgNPs and AO in the FRET system. This method showed a good dynamic range for the target analytics that it established for high quenching efficiency.

The effect of 6-TG on the fluorescence intensity of the AO–AgNPs cluster was investigated further in the presence of an acetate buffer (pH 5.0) at room temperature. Figure 3 shows that 0.57 μM of AO showed a strong fluorescent signal at 525 nm. When another 3.0×10^{-4} μM of AgNPs was mixed into the solution, the fluorescence intensity was reduced due to the adsorbance of AO on the AgNPs' surface. Thus, the fluorescence was quenched. The HR-TEM images of the absence and presence of OA are shown in Fig. 1a. When 0.03 μM of 6-TG was added to the AO–AgNPs mixture, the fluorescent intensity was restored, which shows that 6-TG displaced AO molecules from the AgNPs' surface. The replacement of the AO–AgNPs bond was facilitated by a 6-TG moiety bound to AgNPs through the S–AgNPs bond. Figure 1b shows the HR-TEM results of AO–AgNPs in the presence of 6-TG, which also provided convincing evidence supporting the greater aggregation of AgNPs in the presence of 6-TG due to van der Waal's attraction forces and a reduced surface charge [34]. The results suggest a proficient interaction between AO–AgNPs and 6-TG. Thus, the AO–AgNPs cluster technique is a highly sensitive fluorescence method for 6-TG.

In the proposed method, the fluorescence intensity of the AO–AgNPs system is strongly influenced by various parameters such as pH, concentration of AgNPs, concentration of AO, and incubation time. Therefore, these parameters should be optimized for the determination of 6-TG. The concentration of AgNPs and 6-TG not only influences the fluorescence intensity of the AO–AgNPs assembly but also affects the sensitivity of this system.

The effect of AO was observed (concentration range of 0.17–0.62 μM), which is essential for adsorption on the AgNPs' surface. In our study, this result shows that the fluorescence intensity of AO was magnificently quenched at a concentration of 0.57 μM. All the AO particles were found to be adsorbed by AgNPs with the strongest enhanced fluorescence at this concentration. The obtained intensity remained constant with increasing AO concentrations. Thus, 0.57 μM was the optimum concentration of AO for use in the assay.

One of the most important factors affecting the system variables is pH [35, 36]. The large effect of pH was investigated (range of 2.0–10.0) by addition of 1.0 M NaOH or HCL. The effect of pH depends on the increased fluorescence intensity of the AO–AgNPs conjugate in the presence of 6-TG. The highest response was obtained in the presence and absence of 6-TG at pH ~5.0. Thus, the pH ~5.0 is optimum for further studies (Fig. 4).

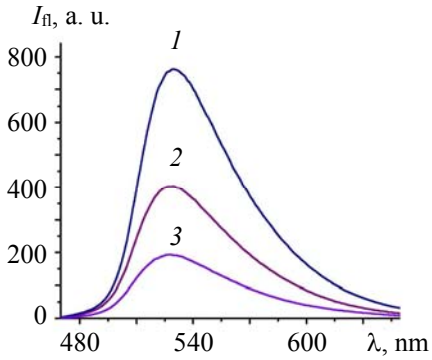

Fig. 3. Fluorescence spectra of (1) AO (0.57 μM), (2) AO–AgNPs (3.0×10^{-4} μM), and (3) AO–AgNPs– 6-TG (0.03 μM).

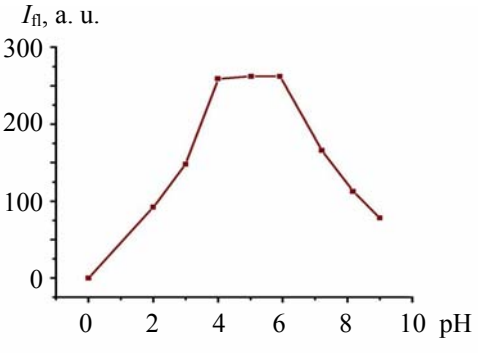

Fig. 4. Effect of pH on the enhanced fluorescence intensity of the AO–AgNPs system in the presence of 6-TG (0.03 μM), AO = 0.57 μM, AgNPs = 3.0×10^{-4} μM.

However, the effect of AgNPs concentration in the recovery of fluorescence using 6-TG was also tested in the range of $(1.0–3.5)\times10^{-5}$ μM (Fig. 5a). The concentration of AgNPs was gradually increased with enhanced fluorescence intensity and remained constant at 3.0×10^{-5} μM, which was optimal for the whole experiment. After increasing the concentration of AgNPs, the efficient response of the fluorescence enhancement decreased because AgNPs are responsible for the collision quenching of the released AO.

Incubation time played a large role in the reaction of dye, AgNPs, and drug. The incubation time was recorded in each 3.0 min interval and investigated (range 2–25 min). An optimal result was obtained at a 15-min reaction. As the time increased, the fluorescence absorbance remained constant; therefore, 15 min was the optimum time for a complete reaction.

Figure 5b shows various concentrations of 6-TG and its effect upon the fluorescence intensity of AO–AgNPs in the FRET system. In the experimental testing process, the fluorescence intensity of AO–AgNPs increased gradually with increasing concentrations of 6-TG (range 0.005–0.04 μM). 6-TG was measured under optimal conditions in a linear dynamic range; i.e., the elevated fluorescence intensity (ΔF) clearly exhibited a good linear response to the 6-TG concentration. A 0.03 μM concentration of the drug was finalized as the optimal concentration for use in the assay (Fig. 5b). The detection limit was 5.3 nM. The relative standard deviation (RSD) of the method was ±0.5048% for five independent measurements of 6-TG. Therefore, the cluster of AO–AgNPs and its response for the detection of 6-TG are highly valuable. Table 1 compares the present method with other existing methods. The results clearly indicate that the current sensor has a very small detection limit amount in comparison to the reported amount.

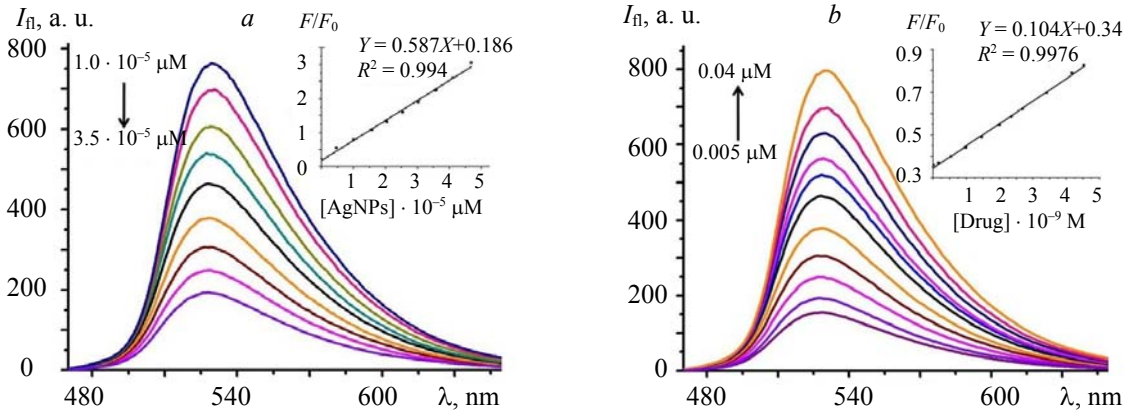

Fig. 5. Fluorescence spectra of (a) AO (0.57 μM) is quenching by increasing AgNPs concentration. pH 5.0, λ_{ex} = 450 nm, and (b) AO–AgNPs system in the presence of different 6-TG concentrations, pH 5.0 (AO = 0.57 μM, AgNPs 3.0×10^{-4} μM); inset is Stern-Volmer calibration graph.

TABLE 1. Comparisons of the Performance of the Present Method for the Determination of 6-TG with Previously Reported Methods

Methods	Linear range, μM/l	LOD, nM	Reference
Voltammetric	0.01–100	8.5	[2]
HPLC	0.8–1.7	400	[7]
SERS	0.1–15.0	65	[11]
LSPR	0.1–10.02	10	[14]
SPR	0.02–1.0	15	[15]
Fluorescence	0.005–0.04	5.2	Present work

N o t e. SPR – surface plasmon resonance, HPLC – high-performance liquid chromatography, SERS – surface-enhanced Raman scattering, LSPR – localized surface plasmon resonance.

Calibration curves were prepared for 6-TG (range 0.005–0.04 μM) under optimal conditions (Fig. 5b). A linear relationship was obtained between the enhanced fluorescence intensity ($\Delta F = F/F_0$) and the 6-TG concentration using the following calibration equation:

$$F/F_0 = 1.04 \times 10^{-10} C_{6\text{-TG}} + 0.34, \; R^2 = 0.9976.$$

A calibration curve was prepared in optimized conditions for 6-TG by a series of prepared solutions. The detection limit was 5.3 nM and the RSD = ±0.5048% for the determination of 6-TG.

A good chemosensor is required for very selective determination of 6-TG [35]. The determination of 6-TG is affected by many interferences due to the presence of cations, anions, and some organic compounds as shown in the determination of 5.3 nM 6-TG. The effect of the most-relevant coexisting constituents such as Na^+, K^+, Mg^{2+}, PO_4^{3-}, Ca^{2+}, Zn^{2+}, Cl^-, and Fe^{2+} on the fluorescence intensity with 0.03 μM 6-TG was studied.

The proposed experiment was applied to determine 6-TG in biological samples, such as urine, serum, and blood using the spiking method (Table 2) to produce a statistical output. The samples were obtained from a private pathology lab in Raipur (Chhattisgarh, India). A greater interference was observed in the determination of 6-TG due to the matrix present in urine, serum, and blood samples. The obtained fluorescence recoveries (range 96.2–102.6%) suggest that further exploration is feasible and has great potential.

TABLE 2. Analytical Results for the Real Samples (n = 5)

Sample	Added, μM	Found, μM	Recovery, %	RSD (±%)
Urine	0.05	0.049(±.04)	99.4	0.5678
	0.5	0.521(±.02)	101.3	0.4231
	1.0	1.041(±.01)	102.6	1.1610
Serum	0.05	0.056(±.03)	100.3	0.6230
	0.5	0.493(±.01)	96.9	0.4311
	1.0	0.973(±.02)	96.2	0.8231
Blood	0.05	0.048(±.02)	97.3	1.0230
	0.5	0.516(±.02)	101.8	0.9311
	1.0	0.983(±.04)	96.2	0.8231

Conclusions. The proposed work developed a novel fluorescent tool for the determination of 6-TG. Conjugated AO–AgNPs were obtained. The addition of 6-TG induced the aggregation of AgNPs, and AO escaped from the surface of AgNPs. The whole mechanism was demonstrated by HR-TEM analysis and applied in the determination of 6-TG in biological samples, such as urine, serum, and blood.

Acknowledgments. The authors thank the CRF laboratory of IIT Kharagpur for HR-TEM analysis and National Institute of Technology, Raipur for providing necessary facilities.

REFERENCES

1. T. P. Huynh, A. Wojnarowicz, M. Sosnowska, S. Srebnik, T. Benincori, F. Sannicolo, F. D'Souza, W. Kutner, *Biosens. Bioelectron*, **70**, 153–160 (2015).
2. A. A. Ensafi, H. Karimi-Maleh, *J. Electroanal. Chem*., **640**, 75–83 (2010).
3. Munshi, N. Pashna, M. Lubin, J. R. Bertino, *Oncologist,* **19**, 760–765 (2014).
4. H. Beitollahi, S. G. Ivari, M. T. Mahani, *Mater. Sci. Eng. C*, **69**, 128–133 (2016).
5. Q. Gueranger, F. Li, M. Peacock, A. Larnicol-Fery, R. Brem, P. Macpherson, J. M. Egly, P. Karran, *J. Invest. Dermatol.*, **134**, 1408–1417 (2014).
6. M. T. Osterman, R. Kundu, G. R. Lichtenstein, J. D. Lewis, *Gastroenterology*, **130**, 1047–1053 (2006).
7. R. Zakrzewski, *J. Anal. Chem.*, **64**, 1235–1241 (2009).
8. B. B. Prasad, R. Singh, A. Kumar, *Carbon*, **102**, 86–96 (2016).
9. U. Hindorf, M. Lindqvist, C. Peterson, P. Soderkvist, M. Strom, H. Hjortswang, *Inflamm. Bowel Dis*., **55**, 1423–1431 (2006).
10. G. Cangemi, A. Barabino, S. Barco, A. Parodi, S. Arrigo, G. Melioli, *Int. J. Immunopathol. Pharmacol.*, **25**, 435–444 (2012).
11. H. Li, X. Chong, Y. Chen, L. Yang, L. Luo, B. Zhao, Y. Tian, *Colloids Surf. A*, **493**, 52–58 (2016).
12. Jacobsen, J. H. Schmiegelow, K. Nersting, *J. Chromatogr. B*, **881-882**, 115–118 (2012).
13. S. A. Coultharda, P. Berry, S. McGarrity, A. Ansari, Christopher P. F. Redfern, *J. Chromatogr. B*, **1028**, 175–180 (2016).
14. N. Bi, M. Hu, H. Zhu, H. Qi, Y. Tian, Hanqi Zhang, *Spectrochim. Acta A*, **107**, 4–30 (2013).
15. X. Y. Deng, Y. Tang, L. H. Wu, L. J. Liu, X. Wang, Y. H. Chen, H. Q. Zhang, Y. Tian, *Chin. J. Anal. Chem.*, **37**, 79 (2009).
16. P. D. Tzanavaras, D. G. Themelis, A. Economou, *Anal. Chim. Acta*, **505**, 167–171 (2004).
17. W. Wang, S. F. Wang, F. Xie, *Sens. Actuat. B*, **120**, 238–244 (2016).
18. M. Amjadi, L. Farzampour, *J. Lumin.*, **29**, 689 (2014).
19. E. Mozioglu, M. Akgoz, T. Kocagoz, C. Tamerler, *Anal. Methods*, **8**, 4017–4021 (2016).
20. Shi, Jingyu, F. Tian, J. Lyu, M. Yang, *J. Mater. Chem. B*, **35**, 6989–7005 (2015).
21. J. N. Miller, *Analyst*, **130**, 265–270 (2005).
22. P. Blaszkiewicz, M. Kotkowiak, A. Dudkowiak, *J. Lumin*., **183**, 303–310 (2017).
23. Y. Chen, L. Chen, Y. Ou, L. Guo, F. Fu, *Sens. Actuat. B: Chem*., **233**, 691–696 (2016).
24. Y. L. Xu, X. Y. Niu, H. J. Zhang, L. F. Xu, S. G. Zhao, H. L. Chen, X. G. Chen, *J. Agric. Food Chem*., **63**, 1747–1755 (2015).
25. F. Gao, Q. Ye, P. Cui, X. Chen, M. Li, L. Wang. *Anal. Methods*, **3**, 1180–1185 (2011).

26. K. H. Lee, S. J. Chen, J. Y. Jeng, Y. C. Cheng, J. T. Shiea, H. T. Chang, *Colloid Interface Sci*., **307**, 340 (2007).
27. P. Liu, Y. Zhou, M. Guo, S. Yang, *Nanoscale*, **10**, 848–855 (2018).
28. N. Y. Chena, H. F. Lia, Z. F. Gaoa, F. Qub, N. B. Lia, H. Q. Luoa, *Sens. Actuat. B: Chem*., **193**, 730–736 (2014).
29. W. Leesutthiphonchai, W. Dungchai, W. Siangproh, N. Ngamrojnavanich, O. Chailapakul, *Talanta*, **85**, 870–876 (2011).
30. U. P. Raghavendra, J. Thipperudrappa, M. Basanagouda, R. M. Melavanki, *J. Lumin.*, **172**, 139–146 (2016).
31. L. Farzampour, M. Amjadi, *J. Lumin*., **155**, 226–230 (2014).
32. S. Qadri, A. Ganoe, Y. Haik, *J. Hazard. Mater*., **169**, 318–323 (2009).
33. J. R. Lakowicz, *Principles of Fluorescence Spectroscopy*, Kluwer, New York (1999).
34. G. L. Wang, W. M. Dong, X. Y. Zhu, W. J. Zhang, C. Wang, H. J. Jiao, *Analyst*, **136**, 5256–5260 (2011).
35. H. C. Dai, Y. Shi, Y. L. Wang, Y. J. Sun, J. T. Hu, P. J. Ni, *Sens. Actuat. B: Chem*., **202**, 201–208 (2014).
36. A. M. E. Badawy, T. P. Luxton, R. G. Silva, K. G. Scheckel, M. T. Suidan, T. M. Tolaymat, *Environ. Sci. Technol.*, **44**, 1260–1266 (2010).